53rd AIAA/ASME/ASCE/AHS/ASC Structures, Structural Dynamics and Materials Conference
20th AI
23 - 26 April 2012, Honolulu, Hawaii

AIAA 2012-1707

Modeling Flutter Response of a Flexible Morphing Wing for UAV

Farhad Sabri[1] and S.A. Meguid.[2]
Mechanics and Aerospace Design Laboratory, University of Toronto, Toronto, ON, M5S 3G, Canada

Aouni A. Lakis[3]
Ecole Polytechnique de Montreal, Montreal, Québec, Canada

This paper is concerned with flutter instability of a novel morphing wing at low mission speeds for different morphing configurations. In view of the flexibility of the wing, it is highly desirable to determine the conditions that trigger flutter instability. Flutter boundary was predicted using the p-k method. Structural dynamics of the wing is obtained using lumped mass method and unsteady aerodynamic using the strip model is used to evaluate corresponding aerodynamic forces and moments. The results indicate that the newly designed flexible concept of the morphing wing increases the critical flutter velocity.

I. Introduction

MORPHING wing is an adaptive wing structure which can change its external shape substantially during the different flight missions. It promises improvements in aircraft maneuverability and aerodynamic performance [1-4]. This has led to considerable research efforts by the community in morphing wing design and analysis. Some recent work concerning morphing wing design, prototype fabrication and the different techniques adopted in developing adaptive wings can be seen in the review provided in Ref. [5]. Recent developments indicate that unmanned aerial vehicle (UAV) using conventional discrete control surfaces (e.g. flap and slats) cannot be sustained because of limited performance and the added weight penalty. On the contrary, multifunctional smart materials such as shape memory alloys (SMA) or piezoectuators can be used as actuators and structural elements partially supporting the aerodynamic loads. The result is a seamless adaptive wing. A novel morphing wing has been developed in our laboratory for UAV that makes use of shape memory alloys. It changes wing configuration by shearing deformation; reducing its effective area; in a desired morphing cycle, as shown in Fig. 1. In a conventional fixed wing configuration, aeroelastic instabilities are an important factor that governs wing design. This fact is also true for a morphing wing in which the wing structure can be flexible. This flexibility may lead to loss of stability even though it is flying at low speed at which a conventional fixed wing aircraft would fly safely. It is therefore the objective of this work to develop a numerical approach to predict flutter onset and the time history of the aeroelastic response due to the coupling between inertial, aerodynamics forces and the structural properties of the UAV.

II. Structural Modeling

The structural dynamic model is obtained by discritizing the wing surface to n mass m_i connected to each other through weightless elastic beam; as depicted in Fig. 2. Each segment has three elastic motions, q_i , q_{n+i} and q_{n+i} corresponding to in-plane and out of-plane bending and elastic rotation, respectively. The kinetic energy and potential energy due to the elastic deformation of the system can be expressed

$$T = \frac{1}{2}\sum_{i=1}^{n} m_i \left(\dot{q}_i^2 + \dot{q}_{i+n}^2 \right) + \frac{1}{2}\sum_{i=1}^{n} I_i \left(\dot{q}_{2n+i}^2 \right) \tag{1}$$

$$U = \frac{1}{2}\sum_{i=1}^{n}\sum_{j=1}^{n} K_{ij}^{In} q_i q_j + \frac{1}{2}\sum_{i=1}^{n}\sum_{j=1}^{n} K_{ij}^{Out} q_{n+i} q_{n+j} + \frac{1}{2}\sum_{i=1}^{n}\sum_{j=1}^{n} K_{ij}^{R} q_{2n+i} q_{2n+j}$$

[1] Postdoctoral Fellow, Department of Mechanical and Industrial Engineering, 5 King's College Rd, AIAA Member.
[2] Professor, Department of Mechanical and Industrial Engineering, 5 King's College Rd, AIAA Lifetime Senior Member.
[3] Professor, Department of Mechanical Engineering 2500 Chemin de Polytechnique.

(2)

where K^{In} and K^{Out} are the fore-and-aft bending stiffness matrix and K^{R} is the torsional stiffness matrix of the wing respectively [6]. Applying the principle of virtual work, using the standard Lagrange's equation of motion in terms of a generalised coordinates system, we obtain the following governing equations:

$$m_i \ddot{q}_{n+i} + \sum_{j=1}^{n} K_{ij}^{In} q_{n+j} = F_x^i \quad ; \quad i = 1,...n \tag{3}$$

$$m_i \ddot{q}_i + \sum_{j=1}^{n} K_{ij}^{Out} q_j = F_z^i \quad ; \quad i = 1,...n \tag{4}$$

$$I_i \ddot{q}_{2n+i} + \sum_{j=1}^{n} K_{ij}^{R} q_{2n+j} = M_y^i \quad ; \quad i = 1,...n \tag{5}$$

The force and moments acting on the wings are discussed in the following section.

III. Aerodynamic Modeling

The surface of the wing in this model is divided into a finite number of two dimensional strips (see Fig. 3). The aerodynamic forces (and moments) are the combination of steady, quasi-steady and unsteady forces acting on each strip, where their components in *X* and *Z* directions can be written as:

$$F_x^i = L_i \sin(\theta_i) + D_i \cos(\gamma_i) \tag{6}$$

$$F_z^i = L_i \cos(\theta_i) + D_i \sin(\gamma_i) - W_i \tag{7}$$

where L_i , D_i and M_y^i are the respective lift, drag and pitching moment and W_i is the weight of each segment. The total lift according to [7]is equal to:

$$\begin{aligned} L_i\ t\ =\ 1/2\ \rho U_\infty A_i\ U_\infty C_{L_\alpha}^i\ \theta_i^e + \pi b_i \dot{\theta}_i \\ - C_{L_\alpha}^i C\ k_i\ \left[\dot{q}_i - U_\infty \theta - \ 1/2\ b_i \dot{\theta}_i\right] - \ 1/2\ \rho A_i b_i \pi \ddot{q}_i \end{aligned} \tag{8}$$

where $C(k_i)$ is the Theodorsen function and k_i is a complex reduced frequency:

$$C(k_i) = \frac{K_1(k_i)}{K_1(k_i) + K_0(k_i)} \tag{9}$$

and the functions $K(k)$ are modified Bessel functions. To account for three dimensional aerodynamic effects of the drag force, including induced drag on the strips, use is made of the expression provided by:

$$D_i = \ 1/2\ \rho U_\infty^2 A_i\ C_{D_0} + C^i_{D_{induced}} \tag{10}$$

and the expression for induced drag is

$$C^{i}_{D_{induced}} = \frac{C^{i^2}_{L_\alpha}\ \theta^{e}_{i} + \theta_i - \ \dot{q}_i / U_\infty}{\pi e A} \tag{11}$$

and the moment about the center of the aerodynamic strip is expressed by,

$$\begin{aligned} M^{y}_{i} = \ 1/2\ \rho U^{2}_{\infty} A_i b_i \left[C^{i}_{M_0} + \ 1/2\ C^{i}_{L_\alpha} \theta^{e}_{i} \right] + \ 1/2\ \pi \rho A_i b_i \left[- \ 1/2\ U_\infty \dot{\theta}_i \right. \\ \left. - \ 1/8\ b^{2}_{i} \ddot{\theta}_i \right] + \ 1/4\ \rho U_\infty A_i b_i C\ k_i\ C^{i}_{L_\alpha} \left[-\dot{q}_i + U_\infty \theta + \ 1/2\ b_i \dot{\theta}_i \right] \end{aligned} \tag{12}$$

IV. Aeroelastic Model

The aeroelastic governing equations of motion are found from combining aerodynamic and structural modeling equations, such that:

$$M\ddot{\chi} + C(\rho, U_\infty, \theta^e)\dot{\chi} + K(\rho, U_\infty, \theta^e)\chi - Q(\rho, U_\infty, \theta^e) = 0 \tag{13}$$

where the unsteady terms of the aerodynamic forces are included in the matrix Q . To predict the flutter boundaries an oscillatory motion is assumed leading to the eigenvalue problem. In this study 'pk' method is applied to evaluate the unsteady forces.

V. Results

The wing planform is rectangular in shape (see Fig. 4) with the specifications listed in Table 1. First, a validation study was performed for the classical Goland's wing to compare the result of present study with other existing data in the literature. Flutter boundaries for our discritized wing, using 10 lumped masses, was compared with Refs. [8, 9] in Table 2. In spite of the fact that they used of different aerodynamic and structural modeling than the ones adopted herein, there is good agreement with our model.

Figure 5 illustrates the complex eigen frequencies for the first bending and torsion modes versus the free stream velocity of unmorphed wing. For the case where there is no free-stream they are pure imaginary quantities representing the respective natural frequencies of 11.84 Hz and 16.31 Hz for flexural and twist modes. By increasing the flight velocity from zero, they become complex (with real and imaginary parts) where the imaginary part represents the frequency of the wing during flight, while the real part represents the damping of the wing. When there is a crossed zero for damping, the corresponding velocity is called the critical flutter velocity where for the unmorphed configuration it is predicted to be 38 m/s. It is also indicating that for higher values of flight velocity, the first flexural mode frequency becomes zero and the wing loses its stability through divergence at 71 m/s.

In order to clarify the improvement resulting from morphing on the aeroelastic behavior of the wing, complex eigen frequencies for a morphed configuration of the wing (backward swept angle equal to 30 degree and area reduction to 30%) are plotted in Fig. 6 for different flight velocity. It is seen that in this case that the flutter onset occurs at flight velocity equal to 47.5 m/s. For different morphing configuration, this flutter velocity is found and listed in Table 3. It is clear that the increase in the swept angle and area reduction leads to higher flutter velocity.

VI. Conclusion

This proposed aeroelastic analysis can predict the flutter instability of the morphing wing during flight. The obtained results provide a good physical insight into the behavior of the morphed wing under different loading conditions and morphed configurations. These results are useful in the design of a flight controller and actuation system for unmanned aerial vehicles travelling at low Reynolds number. Finally, the newly designed morphing wing demonstrates its merits in terms of increase in its divergence and flutter velocities.

Acknowledgments

The authors acknowledge the financial support of the Fonds de Recherche Nature et Technologies (FQRNT), Quebec, Canada and DSO National Laboratories, Singapore.

References

[1] Bae, J.-S., Seigler, T. M., and Inman, D. J., "Aerodynamic and static aeroelastic characteristics of a variable-span morphing wing." Journal of Aircraft, Vol. 42, No.2, 2007, pp. 528-534.

[2] Monner, H. P., "Realization of an optimized wing camber by using form variable flap structures." Aerospace Science and Technology, Vol. 5, No. 7, 2001, pp. 445-455.

[3] Johnston, C. O., Neal, D. A., Wiggins, L. D., Robertshaw, H. H., Mason, W. H., and Inman, D. J., "A model to compare the flight control energy requirements of morphing and conventionally actuated wings.", Collection of Technical Papers - AIAA/ASME/ASCE/AHS/ASC Structures, Structural Dynamics and Materials Conference, Norfolk, VA, United states, 2003, pp. 2862-2870.

[4] Spilman, J., "The Use of Variable Camber to Reduce Drag, Weight and Cost of Transport Aircraft." Aeronautical Journal, Vol. 96, 1992, pp.1-8.

[5] Sofla, A. Y. N., Meguid, S. A., Tan, K. T., and Yeo, W. K. "Shape morphing of aircraft wing: Status and challenges." Materials and Design, Vol. 31, No. 3, 2009, pp. 1284-92.

[6] Sabri, F., Meguid, S.A., Lakis, A.A., Tan, K.T.: Aeroelastic behaviour of a novel morphing wing using shape memory alloys. International Forum on Aeroelasticity and Structural Dynamics, Paris, France (2011).

[7] Van Schoor, M. C., and Von Flotow, A. H., "Aeroelastic characteristics of a highly flexible aircraft." Journal of Aircraft, Vol. 27, No. 10 ,1990, pp. 901-908.

[8] Karpouzian, C., Librescu, L. "Non-classical effects on divergence and flutter of anisotropic swept aircraft wings", AIAA Journal, Vol 34. No.4, 1996, pp. 786-794.

[9] Mazidi, A., Fazelzadeh, S.A. "Flutter of aircraft wings carrying a powered engine under roll maneuver", Journal of Aircraft, Vol. 48, No.3, 2011, pp 874-883.

List of Figures and Tables

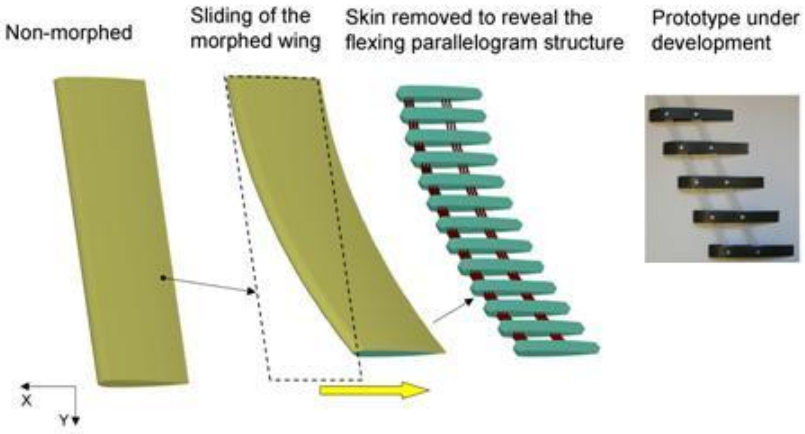

Fig.1- Flexing parallelogram wing box

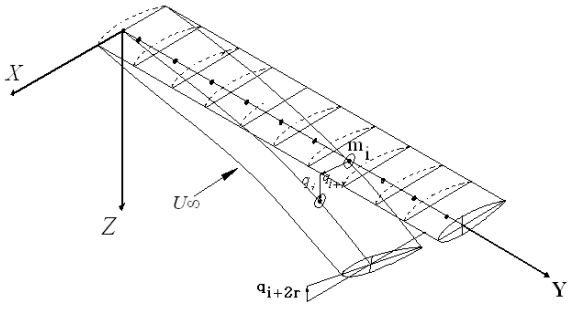

Fig. 2- Lumped mass model of the wing

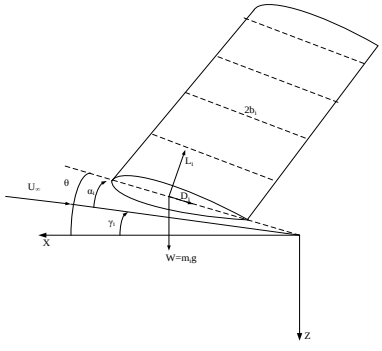

Fig.3 Strip segments for aerodynamic loading

Table 1- Characteristics of UAV morphed wing

Model data	
Half-span	1.70 m
Chord	0.240 m
Mass per unit length	17.65 kg/m
Moment of inertia	0.2 kg m
bending rigidity	8×10^4 N m^2
Torsional rigidity	0.8×10^3 N m^2

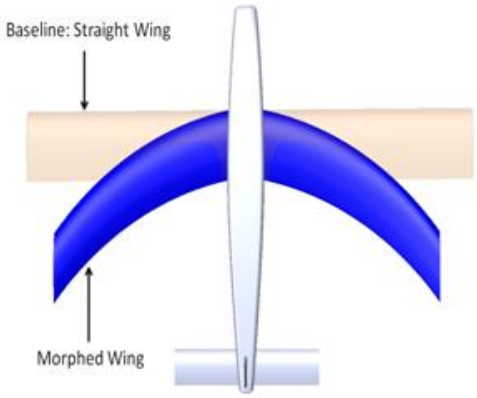

Fig. 4 UAV with Morphing wing

Table2-Nondimensional flutter velocity for Goland's wing

Wing sweep angle, deg	$U_f / b\omega$		
	Ref. [8]	Ref. [9]	Present
0	10.8	10.77	10.93
20	12	11.50	11.29
30	13.3	12.31	13.70

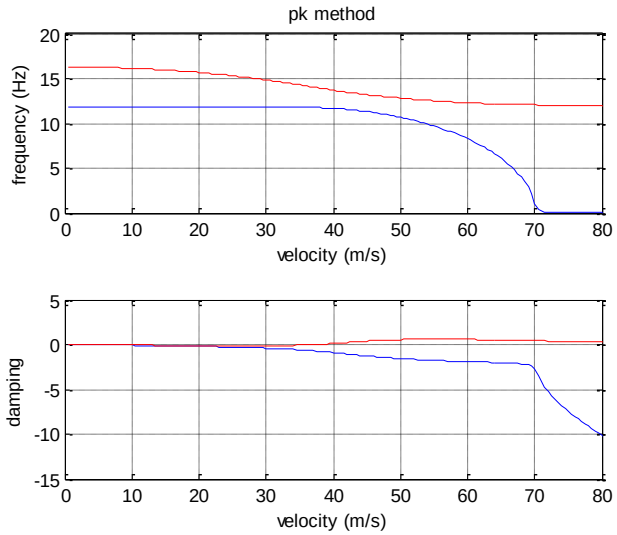

Fig. 5- Eigenvalues of rectangular wing versus freestream velocity

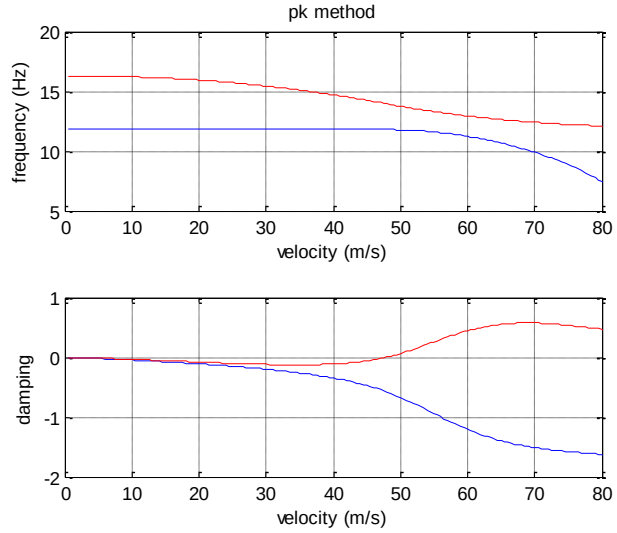

Fig. 6- Eigenvalues of morphed wing versus freestream velocity

Table 3- Effect of Morphing on Flutter boundaries

Wing area reduction (%)	Flutter Velocity (m/s)
0	38
5	40
10	42
15	43
20	43.5
25	45
30	47.5
35	50